

Optimum Thickness and Ug Value of a Hybrid Triple Glazing System with Carbon Dioxide and Vacuum Gaps

Sangchul Kim¹, Sanghoon Baek^{*2}

¹Associate Professor, School of Architecture, Hankyong National University, 327, Jungang-ro, Anseong-si, Gyeonggi-do 17579, Korea.

^{*2}Research Professor, Industry Academic Cooperation Foundation, Hankyong National University, 327, Jungang-ro, Anseong-si, Gyeonggi-do 17579, Korea.
sckim08@hknu.ac.kr¹, shbaek2018@gmail.com^{*2}

Article Info

Volume 83

Page Number: 4073 - 4089

Publication Issue:

March - April 2020

Abstract

This study proposes a hybrid triple glazing system with CO₂ and vacuum gaps and determines its optimum thickness and accompanying heat transmittance (U_g value). The proposed system comprises a typical vacuum section and a CO₂ section, utilizing the greenhouse gas to improve building thermal performance. The optimum thickness of the vacuum section was at 6.2 mm from previous studies. To determine the optimum thickness of the CO₂ section, the U_g value of 120 combinations of glass thicknesses and CO₂ gap were evaluated in 1-mm increments using the THERM & WINDOW programs.

System: The U_g value decreased rapidly with increasing CO₂ gap for all glass thicknesses, up to a CO₂ gap of 10 mm, after which no change was observed. The U_g value reduction ratio for the 1–10 mm thick glass was 14.11–14.38% when the CO₂ gap was increased from 1 to 10 mm, with the 6–7 mm glass thickness exhibiting the greatest reduction ratio of 14.38%. Therefore, the optimum thickness of the proposed hybrid triple glazing system is 22.2–23.2 mm, comprising a 16–17-mm thick CO₂ section and 6.2-mm thick vacuum section, with a U_g value of 0.274 W/m²·K. The optimum thickness of the CO₂ gap and total thickness of the glazing system and U_g value will need to be slightly adjusted depending on the results of future experiments.

Keywords: Hybrid triple glazing system, Carbon dioxide (CO₂), U_g value, Vacuum, Heat transmittance

Article History

Article Received: 24 July 2019

Revised: 12 September 2019

Accepted: 15 February 2020

Publication: 26 March 2020

1. Introduction

With growing attention to addressing climate change, the focus on building energy efficiency has been increasing in the field of architectural and material design research. Building efficiency can be improved by, among other measures, improving the heat transmittance (U_g value) of the building envelope. Accordingly, various studies have been conducted to improve the poor U_g value of

traditional building windows in comparison with that of the exterior walls. The main components of a window are the glazing system and the frame system, of which the glazing system is the primary factor dictating the U_g value of the entire window. A typical glazing system comprises glass layers, insulating gas, and edge sealing. Recently, new materials and techniques have been applied to improve the U_g value of such glazing systems, resulting in systems with a U_g value similar to or

better than that of the building envelope [1,2]. To date, glazing systems with excellent U_g values or high performance can be classified into eight types: (1) multilayer glazing (with insulating gas, low-emission coating, and high-insulating edge sealing), (2) suspended glazing, (3) vacuum glazing, (4) electrochromic glazing, (5) photovoltaic glazing, (6) aerogel glazing, (7) phase change material (PCM) glazing, and (8) self-cleaning glazing.

The traditional multilayer glazing system comprises clear glass layers, air gaps, and aluminum edge sealing. However, this type of glazing system is characterized by a considerable amount of heat loss through convection and radiation via the air gap. Additionally, because the edge sealing has a high thermal conductivity, there is a considerable risk of condensation as well as heat loss along the edges of the window. To overcome these shortcomings, a low-emission coating has been applied together with Argon (Ar) or Krypton (Kr) gas. By applying the low-emission coating to the glass surface, the heat transfer due to the radiation between the glass surfaces was considerably reduced [3–9], and by using Ar or Kr gases, the heat transfer due to the convection in the gas gap was also reduced [10,11]. To minimize the heat loss via conduction through the edge sealing, polyisobutylene (PIB) or silicone-based edge sealing materials with low thermal conductivity have been applied instead of high-conductivity materials, such as aluminum. Combined, these measures have improved the U_g value of windows with multilayer glazing systems to as low as $0.7 \text{ W/m}^2\cdot\text{K}$ [1,2].

The suspended glazing system is similar to the multilayer glazing system; however, an additional thin insulating film is inserted into the gas gap to reduce the U_g value of the window without increasing the thickness of the glazing. Using this technique, a glazing system with a lower U_g value and smaller size and weight can be provided. The suspended glazing system can contribute to considerable energy savings in an office or a high-

rise building with a building envelope made of curtain walls. Among the results reported in recent studies, the lowest U_g value obtained for a suspended glazing system was $0.28 \text{ W/m}^2\cdot\text{K}$ [12,13]. The vacuum glazing system is a unique technology that does not use any insulating gas in the gap between the glass layers. Because the system provides a vacuum gap between the glass layers, heat loss by convection and conduction through the gap is negligible. Moreover, because there is no insulating gas, the gap between the layers can be as thin as approximately 0.2 mm. Furthermore, the application of an Indium-based edge sealing technique has been observed to considerably reduce the risk of vacuum gap rupture. Although the U_g value of manufactured vacuum glazing systems is $0.7 \text{ W/m}^2\cdot\text{K}$, recent triple vacuum glazing system studies have found that the U_g value can be improved to as low as $0.24 \text{ W/m}^2\cdot\text{K}$ [14–20]. The electrochromic glazing system is a recently developed “smart glazing system” that uses chromogenic materials to control the thermal and optical properties of the glass. By changing the color of the glazing according to the intensity of the external solar radiation, the transmittance of solar radiation through an entire window and, thus, the SHGC (Solar Heat Gain Coefficient) can be controlled. The lowest U_g value reported to date for an electrochromic glazing system is $0.62 \text{ W/m}^2\cdot\text{K}$ [21–23]. The photovoltaic (PV) glazing system can be beneficial in reducing the building energy usage as it combines the window glazing with solar cells to simultaneously act as a shading device, insulator, and energy generation system. Although such a multipurpose glazing system has many advantages, its U_g value is slightly higher than that of other glazing systems, recently reported to be $1.1 \text{ W/m}^2\cdot\text{K}$ [24–26]. The aerogel glazing system contains a layer of silica aerogel between the glazing layers, which provides excellent insulation performance and light transmittance. However, owing to the poor tensile strength and durability of the aerogel, such glazing systems can be easily

destroyed if their inner layer comes in contact with water. Nevertheless, due to its high thermal performance and excellent optical properties, it has attracted a significant amount of attention as a futuristic super-insulating glazing system. The lowest aerogel glazing system Ug value reported to date is 0.4 W/m²·K [27,28]. A PCM is a high-performance heat storage and release material that can maintain a constant temperature for a long time during the phase change between its solid and liquid states. Owing to this feature, PCMs have been used to minimize heat loss from building envelopes and floors [29,30]. Recently, studies that apply such PCMs to glazing systems have been conducted. Because PCMs have a relatively low thermal conductivity in both their solid and liquid states, they can replace adiabatic gas in the gap between the glazing layers. Furthermore, PCMs can minimize heat loss through the glazing system as they prevent the glass surface temperature from changing suddenly due to external environmental factors, such as temperature or solar radiation. Recent studies have reported PCM glazing system Ug values below 0.5 W/m²·K [31,32]. The self-cleaning glazing system includes a titanium dioxide (TiO₂) coating applied to the glass surface. This coating acts a photocatalyst that cleans contaminants attached to the glass surface by combining solar radiation and naturally present water. However, because such self-cleaning glazing systems are focused on maintenance concerns rather than insulation performance, their Ug value is approximately 1.2 W/m²·K, which is slightly higher than other recently developed glazing systems [33–35].

Table 1. Ug value of various glazing systems evaluated in previous studies

No.	Type	Main purpose	Ug value in glazing center (W/m ² · K)
1	Multilayer glazing	Insulation	0.70

2	Suspended glazing	Insulation	0.28
3	Vacuum glazing	Insulation	0.24
4	Electrochromic glazing	Insulation, Shading	0.62
5	Photovoltaic glazing	Insulation, Shading, Power generation	1.10
6	Aerogel glazing	Insulation	0.40
7	PCM glazing	Insulation	0.50
8	Self-cleaning glazing	Insulation, Maintenance	1.20

As presented in Table 1, the Ug values of the high-performance glazing systems reported to date range from 0.24 to 1.20 W/m²·K, with the Ug values of the vacuum and suspended glazing systems being the lowest at 0.24 and 0.28 W/m²·K, respectively. The glazing systems proposed in previous studies achieved their high thermal performances by combining new insulating materials with existing systems, effectively reducing greenhouse gas emissions (especially CO₂) by decreasing building energy consumption. Most such glazing systems have included some type of insulating gas in a gas gap. Noble gases such as Argon, Krypton, or Xenon are typically used as such insulating gases as they exhibit little change in their internal energy with temperature change, and rarely participate in chemical reactions with other substances such as water vapor or organic matter. The insulation performances of these gases improve with increased purity. However, considerable technology is required to capture such gases, remove any impurities, processes them for phase changes, and then store them. For this reason, insulating gases for glazing systems are typically costly and can be difficult to supply in large quantities. Accordingly, in this

study, carbon dioxide (CO₂) is proposed for use as an insulating gas in the gas gap instead of a typical noble gas. As CO₂ is one of the major greenhouse gases contributing to global warming, many countries, including South Korea, have long been developing technologies to capture, process, store, transport, and sequester CO₂. These technologies have been developed to considerable levels and can be used in a wide range of applications. If the insulation performance of CO₂ gas can be demonstrated to be similar to that of currently applied insulating gases, it can be used as the insulating gas in glazing systems. Moreover, the use of CO₂ as the insulating gas in the proposed system can contribute to the reduction of CO₂ emissions by recycling gas otherwise released into the atmosphere or sequestered underground or underwater.

This study proposes a novel hybrid triple glazing system comprising a vacuum gap and a CO₂ gap. Because CO₂ is a major greenhouse gas contributing to global warming, its emission or use is strictly controlled by the United Nations Framework Convention on Climate Change (UNFCCC). However, studies on CO₂ capture and storage (CCS) technology have been recently conducted resulting in the capability to artificially control emitted CO₂ [36,37]. CO₂ could represent a particularly useful gas in window glazing systems or other building insulation systems as the insulation performance of pure CO₂ gas is similar to that of Ar gas [38]. Although there are few architectural elements in a building in which pure CO₂ gas can be applied as a thermal insulation material, multiple-layer glazing systems all require some type of insulation gas. Furthermore, in such glazing systems, the gas gap is completely sealed by the edge sealing technology; hence, there is little risk of the CO₂ gas being released into the atmosphere.

The application of CO₂ gas in window glazing systems presents three potentially major advantages. First, if expensive Ar gas can be

replaced with cheap CO₂ gas with very similar insulation performance in glazing systems, the price of the glazing system can be reduced while maintaining a similarly low U_g value. Second, the glazing system in a building is a critical factor affecting its energy efficiency, and the proportion of the glazing system area to the area of an entire building envelope is substantial. If CO₂ can be applied as an insulation gas in the glazing system, buildings can act like forests by capturing CO₂ rather than emitting it. If glazing systems containing captured CO₂ are applied to many buildings, a considerable amount of CO₂ can be sequestered by buildings. Third, the most common method to treat captured CO₂ is to bury it underground, but this treatment process is expensive due to the need for collection, storage, transportation, and burial processes [39]. However, if a portion of captured CO₂ is sequestered in building components, such as window glazing systems, the need to undertake expensive processes, such as burial, can be reduced.

To develop the proposed hybrid triple glazing system containing vacuum and CO₂ gaps, this study focuses on determining the optimum thickness and heat transmittance (U_g-value) of the glazing system. The results are then compared with the U_g values of the other advanced glazing systems presented in previous studies. For this analysis, the THERM and WINDOW software package, version 7.2, distributed by the Lawrence Berkeley National Laboratory, was used. The general theory for the process of constructing a glazing system using this program and the subsequent derivation of results is described in the "NFRC Simulation Manual" [40] and "Technical and Programming Documentation" [41] of the THERM and WINDOW programs.

2. Materials and Methods

2.1 Materials

Figure 1 shows the structure and characteristics of the proposed hybrid triple glazing system with vacuum and CO₂ gaps. This glazing consists of three glass layers, a CO₂ gap, a vacuum gap with a support pillar, and edge sealing. The glazing can thus be divided into a CO₂ section and a vacuum section, each with different edge sealing systems. There is a total of six glass surfaces between the outside and the inside of the proposed glazing system, as indicated in the figure.

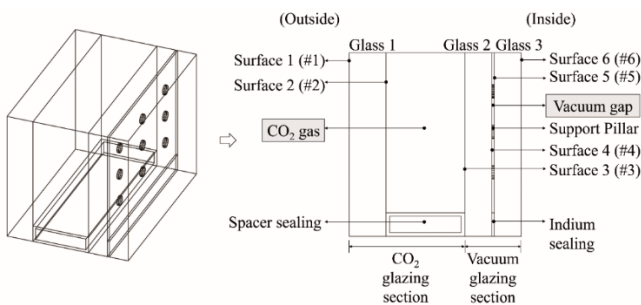


Figure 1. Proposed hybrid triple glazing system with vacuum and CO₂ gaps

In order to determine the optimum thickness of the proposed glazing system, the thicknesses of the CO₂ section and vacuum section must be determined. For the optimum thickness of the vacuum section, the results of previous studies can be used as they have already evaluated the thicknesses of the glass and vacuum gap for optimum Ug values [14–20]. There have not, however, been any previous studies evaluating the thickness of the glass and CO₂ gap for optimum Ug values. Therefore, the main objective of the present study was to determine the optimum thickness of the CO₂ section. The simulation process used to determine the optimum thickness and details of each element in the proposed triple glazing system is described in the following sections.

• **Vacuum section**

The elements of the vacuum section included in the simulation were the two glass layers, vacuum gap, support pillar, and edge sealing. Table 2 shows the thermal and optical properties of the glass applied in this simulation. A 3-mm thick low-conductivity glass was used, and Surface 3 in Figure 1 was coated with a low-emission material. The optical properties of the outdoor facing Surface 6 and indoor facing Surface 3 of the glass are respectively described by T_{sol,1} and T_{sol,2}, which represent the solar radiation transmittance, R_{sol,1} and R_{sol,2}, which represent the solar radiation reflectance, T_{vis,1} and T_{vis,2}, which represent the visible light transmittance, R_{vis,1} and R_{vis,2}, which represent the visible light reflectance, and Emis.1 and Emis.2, which represent the surface emissivity [40].

Table 2. Thermal and optical properties of the glass applied in the proposed glazing system

Field	Input value		
Type	Low-emission glass		
Thickness	3 mm		
Height	1,000 mm		
Conductivity	0.14 (W/m·K)		
Optical characteristics	Solar radiation	Tsol1	0.362
		Tsol2	0.362
		Rsol1	0.553
		Rsol2	0.543
	Visible rays	Tvis1	0.652
		Tvis2	0.652
		Rvis1	0.260
		Rvis2	0.288
Emissivity	Emis.1	0.038	
	Emis.2	0.760	

A 0.2-mm thick vacuum gap was used as suggested in a previous study [18]. Note that because current vacuum glazing methods can only achieve a 99.9% vacuum state, the vacuum gap will always contain a very small amount of air. The vacuum gap also includes a support pillar to prevent damage to the glazing that can result from the pressure difference between the atmosphere and the vacuum [42]. Therefore, although in theory vacuum gaps themselves do not transfer heat other than through radiation, small quantities of heat are transferred through the remaining air and support pillars in such actual glazing systems. Based on this theoretical background, the properties of the vacuum gap applied in the simulation are shown in Table 3.

Table 3. Simulated properties of the vacuum gap

Field	Input value	
Thickness	0.2 (mm)	
Molecular weight of air	28.97 (mol)	
Pressure	0.1332 (Pa)	
Gap heat transfer	0.106787 (W/m ² ·K)	
Support pillar	Type	Circular
	Radius	0.2 (mm)
	Spacing	30 (mm)

Table 4 describes the properties of the edge sealing material used to seal the vacuum gap. In the most common edge sealing method, the vacuum gap was sealed by soldering. However, a new indium edge sealing technology for vacuum gaps has been developed to address the disadvantages of the soldering method [42]. Therefore, indium was used for the edge sealing of the vacuum section in the simulation.

Table 4. Properties of the vacuum gap edge sealing

Type	Material	Width (mm)	Hight (mm)	Conductivity (W/m·K)
Solid	Indium	0.2	15	83.7

• **CO2 section**

The elements of the CO2 section included in the simulation were a single glass layer, the CO2 gap, and edge sealing. The same glass properties applied to the vacuum section were applied to the CO2 section. Table 5 provides the thermal and physical properties of the CO2 gas used in the simulation. These values were obtained at standard atmospheric pressure; the essential values for the simulation are the conductivity, viscosity, and specific heat coefficients according to temperature change, as well as the molecular weight and Prandtl number [40].

Table 5. Thermal and physical properties of CO2 gas at standard atmospheric pressure

Field	Input value	
Type of insulating gas	Carbon dioxide (CO2)	
Molecular weight (mol/g)	44.010	
Pressure (Pa)	101,325	
Prandtl number	0.7808	
	k_{CO2}	0.014567
Conductivity coefficients	A1 (W/m·K)	0.00037
	B1 (W/m·K ²)	0.00002954
	C1 (W/m·K ³)	0.00000008
	μ_{CO2}	0.000014
Viscosity coefficients	A2 (kg/m·s)	0.00000116
	B2 (kg/m·s·K)	0.00000006
	C2 (kg/m·s·K ²)	0
Specific heat	C_{CO2}	827.73413

coefficients	A3	(J/kg·K)	558.8
	B3	(J/kg·K ²)	1.04960001
	C3	(J/kg·K ³)	0.00023876

Based on ISO 15099, the conductivity (k_{CO_2}), viscosity (μ_{CO_2}), and specific heat (C_{CO_2}) of the CO₂ gas in the cavity of the glazing system can be calculated using the following temperature functions, respectively [43,44]:

$$k_{CO_2} = A_1 + B_1 \cdot T + C_1 \cdot T^2, \quad (1)$$

$$\mu_{CO_2} = A_2 + B_2 \cdot T + C_2 \cdot T^2, \quad (2)$$

$$C_{CO_2} = A_3 + B_3 \cdot T + C_3 \cdot T^2, \quad (3)$$

where T is the temperature in degrees Kelvin and A , B , and C are the experimental coefficients.

Table 6 describes the properties of the edge sealing material used to seal the CO₂ gap. The conventional sealing material for a glazing system with an insulating gas gap is an aluminum bar that includes a desiccant. However, recent studies have developed novel sealing technologies using non-metallic and low conductivity materials such as silicone, acryl, polyisobutylene (PIB), or ethylene propylene diene monomer (EPDM), which has been found to improve the rigidity of the edge section in glazing systems due to its superior durability under solar radiation and good adhesion to glass surfaces [45]. According to the results of these studies, an EPDM rubber form was used for CO₂ gap edge sealing in the present study.

Table 6. Properties of CO₂ gap edge sealing

Type	Material	Height (mm)	Conductivity (W/m·K)
Super spacer standard	Flexible EPDM* form	15	0.18

* EPDM: Ethylene propylene diene monomer

• Modeling the hybrid triple glazing

In order to determine the optimum thickness of the proposed hybrid triple glazing system, the optimum thickness of the vacuum section and CO₂ section each need be determined. The thickness of the vacuum section was set to 6.2 mm according to the results of previous studies [14–20]. In order to determine the thickness of the CO₂ section, the thicknesses of the glass and the CO₂ gap were each increased in 1 mm increments in the simulation while the thickness of the vacuum section was maintained, as shown in Figure 2. The thickness range evaluated for the glass was 1–10 mm, the gap range evaluated for the CO₂ gap was 1–12 mm, and each glass thickness was evaluated for each gap, resulting in a total of 120 simulation cases, defined in Table 7.

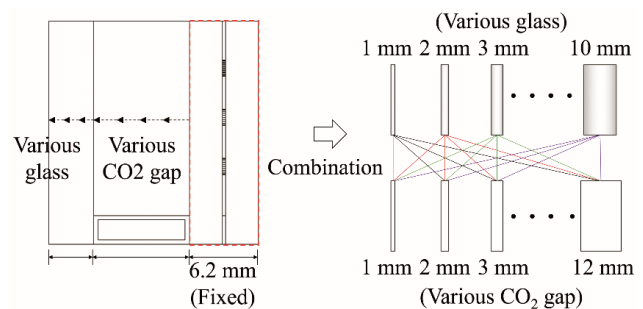


Figure 2. Simulation conditions to determine the optimum thicknesses of the CO₂ section gap and glass layer

Table 7. Simulation cases for determining the optimum thickness of the CO₂ section

Thickness of glass (mm)											
	1	2	3	4	5	6	7	8	9	10	
CO ₂ gap (mm)	1	C. 1	C. 13	C. 25	C. 37	C. 49	C. 61	C. 73	C. 85	C. 97	C. 109
	2	C. 2	C. 14	C. 26	C. 38	C. 50	C. 62	C. 74	C. 86	C. 98	C. 110
	3	C. 3	C. 15	C. 27	C. 39	C. 51	C. 63	C. 75	C. 87	C. 99	C. 111
	4	C. 4	C. 16	C. 28	C. 40	C. 52	C. 64	C. 76	C. 88	C. 100	C. 112
	5	C. 5	C. 17	C. 29	C. 41	C. 53	C. 65	C. 77	C. 89	C. 101	C. 113
	6	C. 6	C. 18	C. 30	C. 42	C. 54	C. 66	C. 78	C. 90	C. 102	C. 114
	7	C. 7	C. 19	C. 31	C. 43	C. 55	C. 67	C. 79	C. 91	C. 103	C. 115
	8	C. 8	C. 20	C. 32	C. 44	C. 56	C. 68	C. 80	C. 92	C. 104	C. 116

2.2 Methods

9 C. 9 C. 21 C. 33 C. 45 C. 57 C. 69 C. 81 C. 93 C. 105 C. 117
10 C. 10 C. 22 C. 34 C. 46 C. 58 C. 70 C. 82 C. 94 C. 106 C. 118
11 C. 11 C. 23 C. 35 C. 47 C. 59 C. 71 C. 83 C. 95 C. 107 C. 119
12 C. 12 C. 24 C. 36 C. 48 C. 60 C. 72 C. 84 C. 96 C. 108 C. 120

C.: Case

Figure 3 illustrates the process of modeling and deriving the results for a 1,000-mm tall hybrid triple glazing system using the THERM and WINDOW software package. First, the “Underlay” function of the software was used to import a DXF file of the glazing design to accurately capture glazing shapes and dimensions. Next, the WINDOW program was used to determine the material properties required by the THERM program, which then used the defined shape and materials to design the glazing system. Once the design of the hybrid triple glazing system was completed, boundary conditions for the indoor and outdoor surfaces of the glazing were entered in order to calculate the U_g value of the system in THERM. The outdoor-facing Surface 1 of the CO₂ section (shown in Figure 1) was set to the outdoor environment in the simulation, while the indoor-facing Surface 6 of the vacuum section was set to the indoor environment. Because the THERM and WINDOW programs analyze the two-dimensional heat flow between two completely different spaces, it was assumed that heat transfer does not occur in the vertical direction [40]. Therefore, the upper and lower ends of the glazing were set to insulation conditions.

The indoor Surface 1 of the glass was divided into a glass edge region that had a large temperature change due to the considerable heat flow at the edges and a glass center region that had a relatively constant temperature. The U_g value was then computed for these two regions [40]. The ranges of the glass edge and center regions were defined according to the Lawrence Berkeley National Laboratory simulation manuals [40,41], which state that although the vertical range of the edge region varies slightly on the glass surface

depending on the edge sealing material, it can generally be defined as being 63.5 mm high. Therefore, in the simulation, the vertical edge region for indoor Surface 1 of the glass was set to 63.5 mm, with the remainder of the glass constituting the center region.

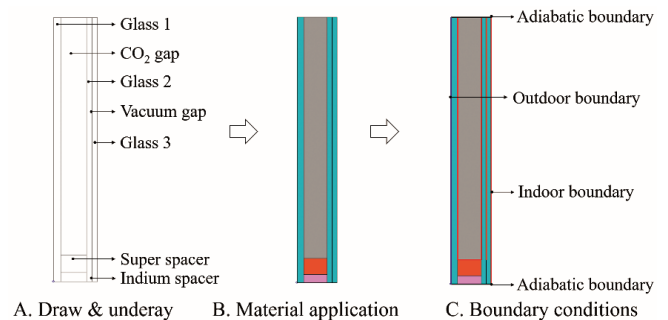


Figure 3. Simulation modeling process to determine the CO₂ section gap and glass thickness

• Indoor and outdoor environmental conditions

Table 8 shows the indoor and outdoor environmental conditions used to calculate the U_g values. These conditions were taken from “KS (Korean Standard) F 2278: Standard test method for thermal resistance for windows and doors,” which is the Korean domestic standard used to calculate the U_g values of glazing systems [46]. The annual average solar radiation used for the U_g value calculation was taken from Korea Standard Weather Data [47].

Table 8. Environmental conditions for indoor and outdoor glass surfaces

	Air temperature	Wind velocity	Convection heat transfer coefficient	Solar radiation
	(°C)	(m/s)	(W/m ² ·K)	(W/m ²)
Indoor	20	1.2	8.8	-
Outdoor	0	4.2	21.2	558

3. Results and discussion

Table 9 shows the U_g values for the 120 evaluated cases of different CO₂ section gas gaps and glass thicknesses with a constant a 6.2-mm thick vacuum section. In order to determine the optimum CO₂ section thickness, the optimum CO₂ gap and glass thickness were determined separately from the data as follows.

Table 9. U_g values of the proposed triple glazing system according to the different CO₂ gap and glass thickness cases evaluated

Thickness of glass (mm)													
		1	2	3	4	5	6	7	8	9	10		
CO ₂ gap (mm)	1	0.324	0.323	0.323	0.322	0.321	0.320	0.320	0.319	0.318	0.318		
	2	0.318	0.317	0.316	0.315	0.315	0.314	0.313	0.313	0.312	0.311		
	3	0.311	0.311	0.310	0.309	0.309	0.308	0.307	0.307	0.306	0.306		
	4	0.306	0.305	0.304	0.304	0.303	0.303	0.302	0.301	0.301	0.300		
	5	0.300	0.300	0.299	0.298	0.298	0.297	0.297	0.296	0.295	0.295		
	6	0.295	0.295	0.294	0.293	0.293	0.292	0.292	0.291	0.290	0.290		
	7	0.290	0.290	0.289	0.289	0.288	0.288	0.287	0.286	0.286	0.285		
	8	0.286	0.285	0.285	0.284	0.284	0.283	0.282	0.282	0.281	0.281		
	9	0.282	0.281	0.280	0.280	0.279	0.279	0.278	0.278	0.277	0.277		
	10	0.278	0.277	0.277	0.276	0.275	0.274	0.274	0.274	0.273	0.273		
	11	0.278	0.277	0.277	0.276	0.275	0.274	0.274	0.274	0.273	0.273		
	12	0.278	0.277	0.277	0.276	0.275	0.274	0.274	0.274	0.273	0.273		

3.1 Determining the CO₂ gap

Figure 4 shows the change in U_g value for different CO₂ gaps from 1 mm to 12 mm according to the thickness of the glass in the CO₂ section with a 6.2-mm thick vacuum section. In previous studies, the U_g value reduction rate with increasing insulating gas gap has exhibited a tendency to decrease when approaching the inflection point, which is often expressed within a certain range. However, in this study, for all glass thicknesses, the U_g value can be

observed to initially decrease rapidly in near linear fashion with increasing CO₂ gap, and when the CO₂ gap reaches 10 mm, the U_g value curve immediately turns horizontally, indicating a clear inflection point after which there is almost no change in the U_g value with increasing CO₂ gap for any glass thickness. Accordingly, it was determined that a CO₂ gap of 10 mm would be most reasonable.

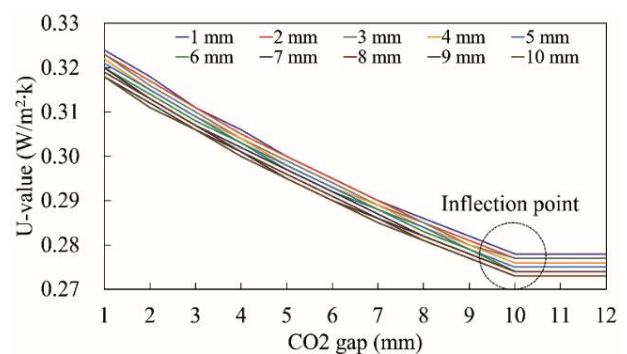


Figure 4. Change in U_g value with CO₂ gap according to glass thickness

3.2 Determining the CO₂ section glass thickness

Figure 5 shows the U_g value reduction ratio for different glass thickness from 1 mm to 10 mm evaluated for CO₂ gaps between 1 mm and 10 mm with a 6.2-mm thick vacuum section. The U_g value for 1-mm thick glass decreased 14.20% as the thickness of the CO₂ gap increased from 1 mm to 10 mm. The U_g values for glass layers 2–10 mm thick decreased between 14.11% and 14.38% as the CO₂ gap increased from 1 mm to 10 mm, with the 6-mm and 7-mm thick glass showing the greatest reduction in U_g value of 14.38%. Therefore, the optimum glass thickness was identified to be either 6 mm or 7 mm.

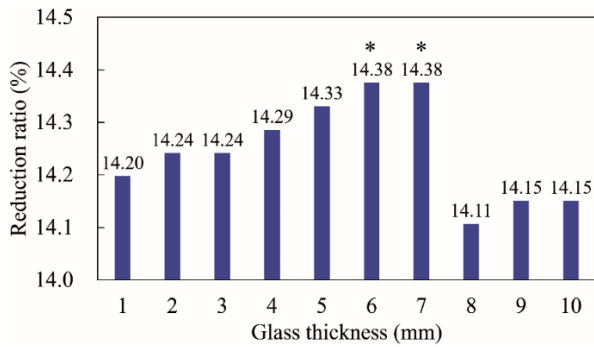


Figure 5. U_g value reduction ratio for different glass thicknesses when increasing the CO₂ gap from 1 mm to 10 mm

3.3 Optimum thickness and U_g value of the proposed hybrid triple glazing system

Figure 6 shows the final design of the proposed hybrid triple glazing system. The vacuum section is 6.2 mm thick, including two 3-mm thick glass layers and a 0.2-mm vacuum gap, and the CO₂ section is 16–17 mm thick, including a 6-mm to 7-mm thick glass layer and a 10-mm CO₂ gap. The total thickness of the evaluated glazing system is therefore 22.2–23.2 mm.

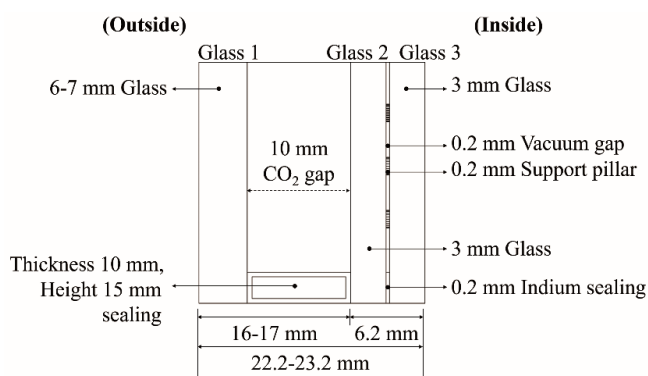


Figure 6. Optimum design for the proposed hybrid triple glazing system

Table 10. Optimum thickness and U_g value for the hybrid triple glazing system

Section	Element	Thickness (mm)	Total thickness (mm)	U _g value (W/m ² ·K)
Vacuum	Glass 3	3.0	6.2	0.274
	Vacuum gap	0.2		
	Glass 2	3.0		
CO ₂	CO ₂ gap	10.0	16.0–17.0	
	Glass 1	6.0–7.0		

Table 10 shows the U_g value and thickness properties of the proposed hybrid triple glazing system according to the final design based on the results in Tables 7 and 9. For combinations C.70 and C.82 in Table 7, representing the 22.2-mm to 23.2-mm thick hybrid triple glazing system consisting of a 6.2 mm thick vacuum section and the 16-mm to 17-mm thick CO₂ section described above, the corresponding U_g value in Table 9 is 0.274 W/m²·K.

3.4 Comparison with U_g values of previous studies

Figure 7 shows a comparison of the U_g values at the center of previous glazing systems and of the proposed hybrid triple glazing system. The U_g value of the proposed hybrid triple glazing system is clearly smaller than the U_g values of the suspended, aerogel, PCM, electrochromic, multilayer, photovoltaic, and self-cleaning glazing systems by 0.006–0.926 W/m²·K. Furthermore, the proposed glazing system provided a U_g value just 0.034 W/m²·K higher than that of the triple vacuum glazing system. Considering these results, it is expected that the proposed hybrid triple glazing system can be successfully used to improve the thermal performance of windows as it exhibits a thermal performance comparable to an existing vacuum glazing system. If the proposed hybrid triple glazing system is fused with solar inhibition systems such as shading, color coating, or

electrochromic glazing, this system can be used to considerably reduce building energy consumption.

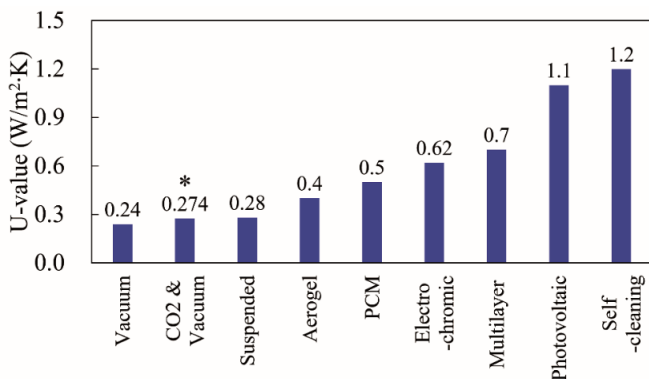


Figure 7. Comparison of Ug values of the proposed hybrid triple glazing system and existing glazing systems

3.5 Improving the Ug value of the proposed hybrid triple glazing system

The Ug value of the proposed hybrid triple glazing system was found to be 0.274 W/m²·K, which is better than most previously proposed glazing systems. However, as shown in Figure 8, a relatively large amount of heat was transferred through the edge sealing part of the vacuum section when compared with the other parts. This seems to be caused by the fact that the edge sealing material in the vacuum section was metal-based, using indium. Indium is a very good material for edge sealing in a vacuum gap because of its excellent adhesion to glass at high temperatures [42]. However, because it has the high thermal conductivity of a metal, its use results in an increase in the Ug value of the glazing system, degrading insulation performance. Therefore, in order to improve the Ug value of the proposed hybrid triple glazing system in future research, it is recommended that efforts be focused on improved vacuum edge sealing technology based on non-metallic materials to reduce such heat transfer.

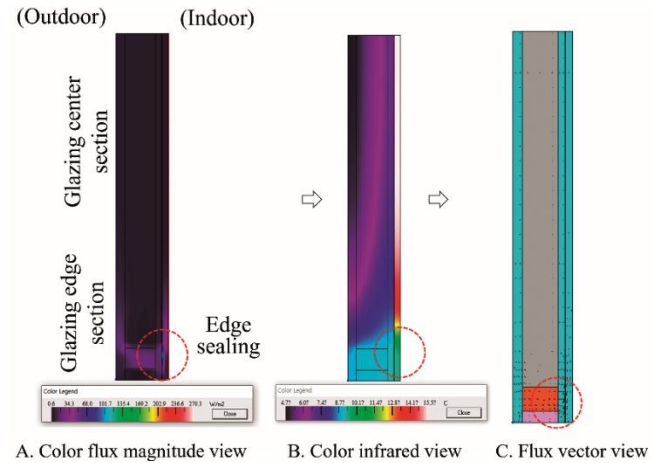


Figure 8. Heat flow through the edge sealing in the vacuum section

3.6 Discussion

As determined in the above analysis, the optimum thickness of the proposed hybrid triple glazing system was 22.2–23.2 mm, and its corresponding Ug value was 0.274 W/m²·K. To simply compare the energy saving performance of the proposed glazing system with that of previous glazing systems, the energy demand of a sample room in which each of the various glazing systems was applied to the exterior wall was analyzed. Figure 9 shows the sample room in which a 4-m wide and 1.5 m-high glazing system was installed on the southern exterior wall. The dates selected to calculate the energy demand were 01 August (0:00–23:00) for summer and 01 December (0:00–23:00) for winter.

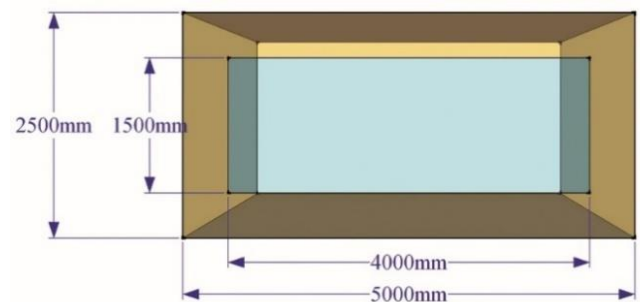


Figure 9. Sample room used to calculate the energy usage according to glazing system

Figure 10 shows the hourly outdoor temperatures on the selected dates [47]. As shown in Table 10, the indoor cooling temperature in summer was set to 26 °C and the indoor heating temperature in winter was set to 20 °C. It was assumed that the operating hours of the cooling and heating units were from 08:00 to 18:00. The hourly cooling and heating load, as well as the associated energy demand, can be calculated using, respectively:

$$Q_g = U_g \cdot A_g \cdot \int_{T_{low}}^{T_{high}} dT \quad (4)$$

$$E_{day} = \sum_{i=8:00}^{i=18:00} Q_{g,i} \cdot h \quad (5)$$

where Q_g , U_g , and A_g are the heat loss (W), heat transmittance (W/m²·K), and surface area (m²) of the glazing system, respectively; T_{high} and T_{low} represent the indoor or outdoor temperatures according to the high-temperature and low-temperature sides, respectively; E_{day} is the energy demand during one day (kWh); and h is the steady state duration, during which a constant temperature was maintained. For the calculation of energy demand, it was assumed that the outdoor temperature was in a steady state (constant temperature) during each hour shown in Figure 10. Finally, it was assumed that there was no heat loss from the room except through the glazing system.

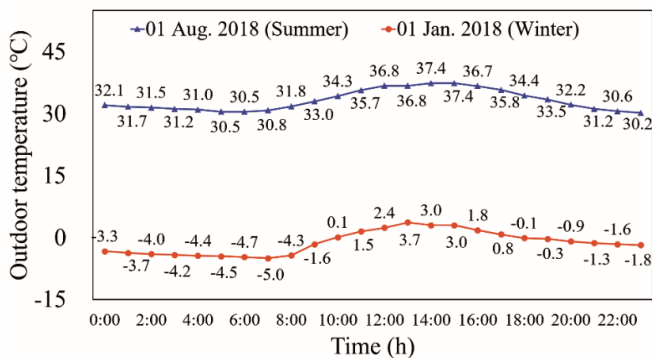


Figure 10. Hourly outdoor temperature on 01 August and 01 January 2018

Table 10. Conditions for indoor cooling and heating

Indoor cooling temperature	26 °C
----------------------------	-------

Indoor heating temperature	20 °C
Unit operating hour	8:00–18:00

Tables 11 and 12 show the hourly energy demand from 8:00 to 18:00 on 01 August (summer) and 01 January (winter), respectively, for each glazing system type, and Figure 11 shows the total energy demand combining the energy consumed under summer and winter conditions. Clearly, the self-cleaning glazing system exhibited the highest energy demand (approximately 2.295 kWh). The energy demands of the photovoltaic, multilayer, electrochromic, PCM, Aerogel, and suspended glazing systems were found to be 2.103, 1.339, 1.186, 0.956, 0.765, and 0.535 kWh, respectively. Notably, the energy demand of the proposed hybrid triple glazing system with CO₂ and vacuum gaps was found to be 0.524 kWh, which was lower than the energy demands of all previously proposed glazing systems except the triple vacuum glazing system. Although the U_g value of the proposed glazing system was approximately 0.034 W/m²·K higher than that of the triple vacuum glazing system, the proposed system still exhibited excellent energy savings performance. Based on these results, the authors plan to fabricate a prototype of the proposed glazing system in the future and conduct a pilot test to measure its actual U_g value in accordance with the ISO 15099 and KS F 2278 standards. Then, the prototype will be installed in a building specially constructed for experiments and the insulation performance, energy performance, and energy cost reduction provided by the proposed glazing system will be investigated under actual summer and winter weather conditions. In particular, as with vacuum glazing systems that have been observed to exhibit considerable discrepancies between experimental and commercial glazing systems due to technical limitations [2], the proposed glazing system is also expected to exhibit discrepancies between the results of theoretical evaluations and experimental

tests. Therefore, as part of this future research, the authors plan to identify the causes of any such discrepancies between theoretical and actual Ug values after the pilot test, and to propose solutions to minimize such errors in the glazing system production process.

Table 11. Hourly energy demand per summer day according to type of glazing system

Time	Triple vacuum	CO2 & vacuum	Suspended	Aerogel	PCM	Electrochromic	Multilayer	Photo-voltaic	Self-cleaning
8:00	8.4	9.5	9.7	13.9	17.4	21.6	24.4	38.3	41.8
9:00	10.1	11.5	11.8	16.8	21.0	26.0	29.4	46.2	50.4
10:00	12.0	13.6	13.9	19.9	24.9	30.9	34.9	54.8	59.8
11:00	14.0	15.9	16.3	23.3	29.1	36.1	40.7	64.0	69.8
12:00	15.6	17.8	18.1	25.9	32.4	40.2	45.4	71.3	77.8
13:00	15.6	17.8	18.1	25.9	32.4	40.2	45.4	71.3	77.8
14:00	16.4	18.7	19.2	27.4	34.2	42.4	47.9	75.2	82.1
15:00	16.4	18.7	19.2	27.4	34.2	42.4	47.9	75.2	82.1
16:00	15.4	17.6	18.0	25.7	32.1	39.8	44.9	70.6	77.0
17:00	14.1	16.1	16.5	23.5	29.4	36.5	41.2	64.7	70.6
18:00	12.1	13.8	14.1	20.2	25.2	31.2	35.3	55.4	60.5
Total (Wh)	149.9	171.1	174.9	249.8	312.3	387.3	437.2	687.1	749.5
Total (kWh)	0.150	0.171	0.175	0.250	0.312	0.387	0.437	0.687	0.750

Table 12. Hourly energy demand per winter day according to type of glazing system

Time	Triple vacuum	CO2 & vacuum	Suspended	Aerogel	PCM	Electrochromic	Multilayer	Photo-voltaic	Self-cleaning
8:00	36.0	41.1	42.0	60.0	75.0	93.0	105.0	165.0	180.0
9:00	35.0	39.9	40.8	58.3	72.9	90.4	102.1	160.4	175.0
10:00	31.1	35.5	36.3	51.8	64.8	80.4	90.7	142.6	155.5

11:00	28.7	32.7	33.4	47.8	59.7	74.0	83.6	131.3	143.3
12:00	26.6	30.4	31.1	44.4	55.5	68.8	77.7	122.1	133.2
13:00	25.3	28.9	29.6	42.2	52.8	65.5	73.9	116.2	126.7
14:00	23.5	26.8	27.4	39.1	48.9	60.6	68.5	107.6	117.4
15:00	24.5	27.9	28.6	40.8	51.0	63.2	71.4	112.2	122.4
16:00	24.5	27.9	28.6	40.8	51.0	63.2	71.4	112.2	122.4
17:00	26.2	29.9	30.6	43.7	54.6	67.7	76.4	120.1	131.0
18:00	27.6	31.6	32.3	46.1	57.6	71.4	80.6	126.7	138.2
Total (Wh)	309.0	352.8	360.5	515.0	643.8	798.3	901.3	1416.4	1545.1
Total (kWh)	0.309	0.353	0.361	0.515	0.644	0.798	0.901	1.416	1.545

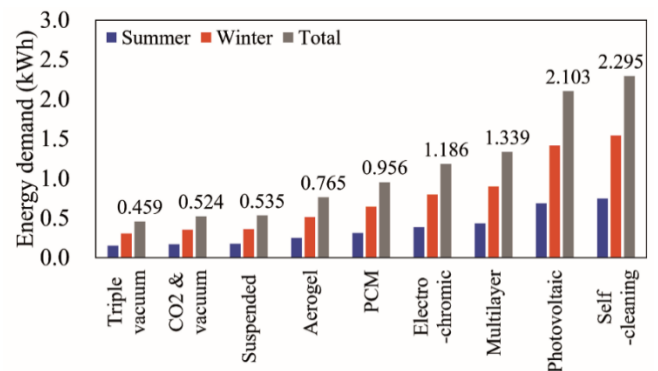


Figure 11. Comparison of total energy demand (summer + winter) according to type of glazing system

4. Conclusions

This study was conducted to evaluate a proposed hybrid triple glazing system with CO2 and vacuum gaps as a technology to utilize CO2, a greenhouse gas (GHG), in glazing systems, and to derive its optimum thickness and Ug value. This study can be summarized as follows.

1. The proposed hybrid triple glazing system is divided into a vacuum section and a CO2 section. An optimum vacuum section thickness of 6.2-mm was applied, including two 3-mm thick glass panels and a 0.2-mm

vacuum gap, according to the results of previous studies. The CO₂ section consisted of one glass layer and one CO₂ gap; this study focused on deriving the optimum thickness of this section. To determine the optimum thickness of the CO₂ section, the glass and CO₂ gap were evaluated over ranges of 1–10 mm and 1–12 mm, respectively. The 6.2-mm thick vacuum section was then combined with the glass and CO₂ gap of the CO₂ section to evaluate 120 hybrid triple glazing systems of different total thicknesses. The U_g values of the 120 glazing systems were calculated using the THERM and WINDOW simulation programs, and then analyzed according to the thickness of the glass and the CO₂ gap.

2. When determining the optimum CO₂ gap, the U_g values of all hybrid triple glazing systems initially decreased as the CO₂ gap increased, regardless of the thickness of the glass. When the CO₂ gap reached 10 mm, an inflection point was observed after which the U_g values no longer decreased, instead remaining constant. In previous studies, the U_g value reduction rate due to an increasing insulating gas gap has shown a tendency to decrease as the inflection point is approached, and the inflection point is often expressed within a certain range. In this study, however, the inflection point was expressed as a single point (10 mm) and the U_g value change rate was also very well defined. This is because the change in the CO₂ gap thickness was set to a relatively large interval (1 mm). In particular, there were limitations in precisely analyzing the change in the U_g value because the computational grid of the THERM and WINDOW software was relatively large. Therefore, a more precise analysis of the optimum CO₂ gap is necessary to compare the actual data from future experiments with analysis data.
3. In the analysis of the optimum CO₂ section glass thickness, when the 6.2-mm thick vacuum section was combined with the 1-mm thick glass and 1-mm thick CO₂ gap, the U_g value of the hybrid triple glazing system was 0.324 W/m²·K. When the 6.2-mm thick

vacuum section was combined with 1-mm thick glass and the optimum CO₂ gap of 10 mm, the U_g value of the triple glazing system decreased by approximately 14.2% to 0.278 W/m²·K. For the same change in CO₂ gap using glass thicknesses between 2 and 10 mm, the 6-mm and 7-mm thick glass exhibited the largest U_g value reduction rate of approximately 14.38% from 0.320 W/m²·K to 0.274 W/m²·K. Therefore, it was determined that the most effective glass thickness when combined with the optimum CO₂ gap of 10 mm is between from 6 mm and 7 mm. The other glass thicknesses were determined to be inefficient in terms of the U_g value reduction rate.

4. Based on these results, it was determined that the optimum thickness of the proposed hybrid triple glazing system is between 22.2 mm and 23.2 mm, combining the 6.2-mm thick vacuum section, 10-mm CO₂ gap, and 6-mm to 7-mm thick glass layer. The U_g value of this configuration was 0.274 W/m²·K. It is likely, however, that the optimum thickness of the CO₂ gap will need to be slightly adjusted depending on the results of future experiments. Therefore, the total thickness of the glazing system and its U_g value will probably change slightly depending on the results of these future experiments.

5. Acknowledgment

This research was supported by Basic Science Research Program through the National Research Foundation of Korea(NRF) funded by the Ministry of Education(2018R1A6A3A01013035)

References

- [1] Jelle, B, Hynd, A, Gustavsen, A, Arasteh, D, Goudey, H, Hart, R. Fenestration of today and tomorrow: a state-of-the-art review and future research opportunities. *Sol. Energy Mater. Sol. Cells* 2012, 96, 1–28. DOI: <https://doi.org/10.1016/j.solmat.2011.08.010>

- [2] Erdem, C, Saffa, B.R. A state-of-the art review on innovative glazing technologies. *Renewable Sustainable Energy Rev.* 2015, 41, 695–714. DOI: <https://doi.org/10.1016/j.rser.2014.08.084>
- [3] Re, M.D, Gouttebaron, R, Dauchot, J.P, Hecq, M. Study of the optical properties of AlN/ZrN/AlN low-e coating. *Surf. Coat. Technol.* 2004, 180-181, 488–495. DOI: <https://doi.org/10.1016/j.surfcoat.2003.10.093>
- [4] Kiyoshi, C, Toshiyuki, T, Takashi, K, Hironori, O. Low-emissivity coating of amorphous diamond-like carbon/Ag-alloy multilayer on glass. *Appl. Surf. Sci.* 2005, 246(1–3). 24–51. DOI: <https://doi.org/10.1016/j.apsusc.2004.10.046>
- [5] Reidinger, M, Rydzek, M, Scherdel, C, Arduini-Schuster, M, Manara, J. Low-emitting transparent coating based on tin doped indiumoxide applied via a sol-gel routine. *Thin Solid Films* 2009, 517, 3096–3099. DOI: <https://doi.org/10.1016/j.tsf.2008.11.078>
- [6] Francesco, A,; Giorgio, B, Theoretical modelling and experimental evaluation of the optical properties of glazing systems with selective films. *Build. Simul.* 2009, 2(2), 75–84. DOI: [10.1007/S12273-009-9112-5](https://doi.org/10.1007/S12273-009-9112-5)
- [7] Jun, H, Lin, L, Hongxing, Y. Numerical evaluation of the mixed convective heat transfer in a double-pane window integrated with see-through a-Si PV cells with low-e coatings. *Appl. Energy* 2010, 87(11), 3431–3437. DOI: <https://doi.org/10.1016/j.apenergy.2010.05.025>
- [8] Han, K, Kim, J. Reflectance modulation of transparent multilayer thin films for energy efficient window applications. *Mater. Lett.* 2011, 65(15–16), 2466–2469. DOI: <https://doi.org/10.1016/j.matlet.2011.05.006>
- [9] Hee, W.J, Alghoul, M.A, Bakhtyar, B, OmKalthum, E, Shameri, M.A, Alrubaih, M.S, Sopian, K. The role of window glazing on daylighting and energy saving in buildings. *Renewable Sustainable Energy Rev.* 2015, 42, 323–343. DOI: <https://doi.org/10.1016/j.rser.2014.09.020>
- [10] Larsson, U, Moshfegh, B, Sandberg, M. Thermal analysis of super insulated windows (numerical and experimental investigations). *Energy Build.* 1999, 29, 121–128. DOI: [https://doi.org/10.1016/S0378-7788\(98\)00041-3](https://doi.org/10.1016/S0378-7788(98)00041-3)
- [11] Erdem C. Accurate and reliable U-value assessment of argon-filled double glazed windows: A numerical and experimental investigation. *Energy Build.* 2018, 171, 100–106. DOI: <https://doi.org/10.1016/j.enbuild.2018.04.036>
- [12] Aritra, G, Brian N. Durability of switching behaviour after outdoor exposure for a suspended particle device switchable glazing. *Sol. Energy Mater. Sol. Cells* 2017, 163, 178–184. DOI: <https://doi.org/10.1016/j.solmat.2017.01.036>
- [13] Qi, L, Yipin, W, Jinyuan, Y, Guifu, D. Impact resistance and static strength analysis of an extremely simplified micro hotplate with novel suspended film. *Sens. Actuators, A* 2018, 208, 495–504. DOI: <https://doi.org/10.1016/j.sna.2018.08.003>
- [14] Papaefthimiou, S, Leftheriotis, G, Yianoulis, P, Hyde, T.J, Eames, P.C, Fang, Y, Pennarun, P-Y, Jannasch, P. Development of electrochromic evacuated advanced glazing. *Energy Build.* 2006, 38, 1455–1467. DOI: <https://doi.org/10.1016/j.enbuild.2006.03.029>
- [15] Yueping, F, Philip, C.E, Brian, N, Trevor, J.H. Experimental validation of a numerical model for heat transfer in vacuum glazing. *Sol. Energy* 2006, 80(5), 564–577. DOI: <https://doi.org/10.1016/j.solener.2005.04.002>
- [16] Manz, H, Brunner, S, Wullschleger, L. Triple vacuum glazing: Heat transfer and basic mechanical design constraints. *Sol. Energy* 2006, 80(12), 1632–1642. DOI: <https://doi.org/10.1016/j.solener.2005.11.003>
- [17] Yueping, F, Philip, C.E, Brian, N, Trevor, J.H, Junfu, Z, Jinlei, W, Ye, H. Low emittance coatings and the thermal performance of vacuum glazing. *Sol. Energy* 2007, 81(1), 8–12. DOI: <https://doi.org/10.1016/j.solener.2006.06.011>
- [18] Philip C.E. Vacuum glazing: Current performance and future prospects. *Vacuum* 2008, 82(7), 717–722. DOI: <https://doi.org/10.1016/j.vacuum.2007.10.017>
- [19] Yueping, F, Trevor, H, Neil, H, Philip, C.E, Brian N. Comparison of vacuum glazing thermal performance predicted using two-and three-dimensional models and their experimental

- validation. *Sol. Energy Mater. Sol. Cells* 2009, 93(9), 1492–1498. DOI: <https://doi.org/10.1016/j.solmat.2009.03.025>
- [20] Yueping, F, Trevor J.H, Neil, H. Predicted thermal performance of triple vacuum glazing. *Sol. Energy* 2010, 84(12), 2132–2139. DOI: <https://doi.org/10.1016/j.solener.2010.09.002>
- [21] Piccolo, A, Pennisi, A, Simone, F. Daylighting performance of an electrochromic window in a small scale test-cell. *Solar Energy* 2009, 83(6), 832–844. DOI: <https://doi.org/10.1016/j.solener.2008.11.013>
- [22] Piccolo, A, Simone, F. Effect of switchable glazing on discomfort glare from windows. *Build. Environ.* 2009, 44(6), 1171–1180. DOI: <https://doi.org/10.1016/j.buildenv.2008.08.013>
- [23] Ruben, B, Bjorn, P.J, Arild, G. Properties, requirements and possibilities of smart windows for dynamic daylight and solar energy control in buildings: A state-of-the-art review. *Sol. Energy Mater. Sol. Cells* 2010, 94(2), 87–105. DOI: <https://doi.org/10.1016/j.solmat.2009.08.021>
- [24] Tady, Y.Y.F, Yang, H. Study on thermal performance of semi-transparent building-integrated photovoltaic glazings. *Energy Build.* 2008, 40(3), 341-350. DOI: <https://doi.org/10.1016/j.enbuild.2007.03.002>
- [25] Henrik, D, Bengt, P, Bjorn, K. System analysis of a multifunctional PV/T hybrid solar window. *Sol. Energy* 2012, 86(3), 903–910. DOI: <https://doi.org/10.1016/j.solener.2011.12.020>
- [26] Erdem, C, Pinar, M.C. Effects of concavity level on heat loss, effectiveness and efficiency of a longitudinal fin exposed to natural convection and radiation. *Int. J. Numer. Methods Heat Fluid Flow* 2013, 23(7), 1169–1178. DOI: <https://doi.org/10.1108/HFF-03-2011-0054>
- [27] Erdem, C, Pinar, M.C, Christopher J.W, Saffa B.R. Optimizing insulation thickness and analysing environmental impacts of aerogel-based thermal superinsulation in buildings. *Energy Build.* 2014, 77, 28–39. DOI: <https://doi.org/10.1016/j.enbuild.2014.03.034>
- [28] Erdem, C, Pinar, M.C, Christopher, J.W, Saffa, B.R. Toward aerogel based thermal superinsulation in buildings: A comprehensive review. *Renewable Sustainable Energy Rev.* 2014, 34, 273–299. DOI: <https://doi.org/10.1016/j.rser.2014.03.017>
- [29] Baek, S, Kim, S. Determination of optimum hot-water temperatures for PCM radiant floor-heating systems based on the wet construction method. *Sustainability* 2018, 10(11), 4004. DOI: <https://doi.org/10.3390/su10114004>
- [30] Baek, S, Kim, S. Analysis of thermal performance and energy saving potential by PCM radiant floor heating system based on wet construction method and hot water. *Energies* 2019, 12(5), 828. DOI: <https://doi.org/10.3390/en12050828>
- [31] IsmailJ, K.A.R, Henriquez, R. Thermally effective windows with moving phase change material curtains. *Appl. Therm. Eng.* 2001, 21(18), 1909–1923. DOI: [https://doi.org/10.1016/S1359-4311\(01\)00058-8](https://doi.org/10.1016/S1359-4311(01)00058-8)
- [32] Mohammed, M.F, Amar, M.K, Siddique, A.K.R, Said A.H. A review on phase change energy storage: materials and applications. *Energy Convers. Manage.* 2004, 45(9–10), 1597–1615. DOI: <https://doi.org/10.1016/j.enconman.2003.09.015>
- [33] Akira, F, Xintong, Z. Titanium dioxide photocatalysis: present situation and future approaches. *C.R. Chim.* 2006, 9(5–6), 750–760. DOI: <https://doi.org/10.1016/j.crci.2005.02.055>
- [34] Raquel, P, Garikoitz, B, Arrate, M, Josu, G, Ana, A. Development of multifunctional sol-gel coatings: Anti-reflection coatings with enhanced self-cleaning capacity. *Sol. Energy Mater. Sol. Cells* 2010, 94(6), 1081–1088. DOI: <https://doi.org/10.1016/j.solmat.2010.02.031>
- [35] Krister, M, Bjorn, P.J. Self-cleaning glazing products: A state-of-the-art review and future research pathways. *Sol. Energy Mater. Sol. Cells* 2013, 109, 126–141. DOI: <https://doi.org/10.1016/j.solmat.2012.09.034>
- [36] Mar, P.F, Andrei, B.D, Evangelos, T. CO2 Utilization Pathways: Techno-Economic Assessment and Market Opportunities. *Energy Procedia* 2014, 63, 7968–7975. DOI: <https://doi.org/10.1016/j.egypro.2014.11.834>
- [37] Sara, B, Samuel, K, Niall, M.D, Nigel, B, Adam, H. An assessment of CCS costs, barriers and potential. *Energy Strategy Reviews* 2018, 22, 61–81. DOI: <https://doi.org/10.1016/j.esr.2018.08.003>

- [38] Baek, S, Park, J.C. Analysis on Thermal Performance of Double-Pane Unit Filled Carbon Dioxide, The Society of Air-conditioning and Refrigerating Engineers of Korea 2015, 2015(6), 220–223.
- [39] Mijndert, V.D.S, Simon, R, Edward, S.R. Best practices and recent advances in CCS cost engineering and economic analysis, Int. J. Greenhouse Gas Control 2019, 83, 91–104. DOI: <https://doi.org/10.1016/j.ijggc.2019.02.006>
- [40] National Fenestration Rating Council, 2017, Therm 7/Window7 NFRC simulation manual. Available Online: <https://windows.lbl.gov/sites/default/files/Downloads/NFRCSim7-July2017.pdf> (Accessed on 25 June, 2019)
- [41] Carli Inc., 2006, Conrad 5 & Viewer 5 Technical and Programming Documentation. Available Online: <https://windows.lbl.gov/sites/all/files/Downloads/conrad-and-viewer-06-20-06.pdf> (Accessed on 25 June, 2019)
- [42] Yueping, F, Trevor, J.H, Farid A, Neil H, Philip C.E, Brian, N, Seth M. Indium alloy-sealed vacuum glazing development and context, Renewable Sustainable Energy Rev. 2014, 37, 480–501. DOI: <https://doi.org/10.1016/j.rser.2014.05.029>
- [43] International Standard, 2012, ISO 15099: Thermal performance of windows, doors, and shading devices-Detailed calculations. Available Online: http://www.questin.org/sites/default/files/intl-codes/et.iso_.15099.2003.pdf (Accessed on 25 June, 2019)
- [44] Lawrence Berkeley National Laboratory, 2019, Window 7 user manual. Available Online: <https://windows.lbl.gov/sites/default/files/software/WINDOW/WINDOW7UserManual.pdf> (Accessed on 25 June, 2019)
- [45] Sofie, V.D.B, Robert, H, Bjorn, P.J, Arild, G. Window spacers and edge seals in insulating glass units: A state-of-the art review and future perspectives, Energy Build. 2013, 58, 263–280. DOI: <https://doi.org/10.1016/j.enbuild.2012.10.006>
- [46] Korean Standard Service Network. Standard test method for thermal resistance for windows and doors. 2017. Available Online: <https://www.kssn.net/search/stdtdetail.do?itemNo=K001010113352> (Accessed on 25 June, 2019)
- [47] Passive House Institute Korea. Republic of Korea Standard Weather Data. 2017. Available Online: http://www.phiko.kr/bbs/board.php?bo_table=z3_01&wr_id=2479 (Accessed on 25 June, 2019)